FRINGE SPACING AND STRAIN ANALYSIS USING LASER MOIRÉ FRINGE PROJECTION TECHNIQUE

By

Setegn Ayalew Bogale

SUBMITTED IN PARTIAL FULFILLMENT OF THE
REQUIREMENTS FOR THE DEGREE OF
MASTER OF SCIENCE IN PHYSICS
AT
ADDIS ABABA UNIVERSITY
ADDIS ABABA, ETHIOPIA
JUNE 2009

ADDIS ABABA UNIVERSITY

DEPARTMENT OF

PHYSICS

Supervisor: _____

Prof. A.V Gholap

Examiners: _____

_____

ADDIS ABABA UNIVERSITY

Date: **June 2009**

Author: **Setegn Ayalew Bogale**

Title: **Fringe Spacing and Strain Analysis Using Laser Moiré Fringe Projection Technique**

Department: **Physics**

Degree: **M.Sc.** Convocation: **June** Year: **2009**

Signature of Author

For those who have unlimited potential but cannot attend the School.

Table of Contents

List of Figures

Abstract

The spacing between fringes is crucial for testing materials based on Moiré technique. In this work, the spacing between two consecutive bright (or dark) fringes, C , is determined, for different grating separation , α. The behavior shows that as the angle between the gratings increases, the fringe spacing decreases. For gratings of 100 lines/mm and 300 lines/mm pitches adjusted parallel to each other, it is confirmed that the fringe spacing equals 0.005000 mm. This is equal to the value for λ_{beat}. Moreover, a moiré fringe projection technique applicable for deformation measurement is done experimentally. The results show that moiré fringe projection technique is suitable for deformation analysis.

Acknowledgement

Above all, I would like to thank the almighty; God, for letting me accomplish this stage.
I am deeply indebted to Prof. A.V Gholap, my supervisor, for his suggestions; constant support and friendly approach during this research.

I would like to thank Mr.Tesfaye Mamo, Mr.Yeneneh Yalew, and Mr.Desalegn Tadesse for their technical and computational assistance. My strongest thank is addressed to Mr.Mulugeta Nida and Mr.Muluken Regassa, GIW chemists; for their kind support in bringing samples. I would like to thank also all my family and friends; without their help this stage was unthinkable. I have derived materials from many research journals and books, especially ICTP e-journal groups; and am indebted to the authors of those publications and books.

Finally, I am also thankful to Mr.Tesfaye Mamuye for his patient support in collecting and sending my salary for the entire two years.

Introduction

Moiré Techniques have been used for a number of testing applications.Righi(1887) first noticed that the relative displacement of two gratings could be determined by observing the movement of the moiré fringes. The next significant advance in the use of moiré was presented by Weller and Shepherd(1948). They used moiré to measure the deformation of an object under applied stress-by looking at the differences in a grating pattern before and after the applied stress. They were also the first to use shadow moiré,where a grating is placed in front of a non flat surface to determine the shape of the object behind it by using the shape of the moiré fringes.

In this extract, fringe spacings, for different grating angle separation, are determined using FORTRAN written program. And also an alternative experimental moiré fringe projection technique applicable for deformation measurement is proposed. Particularly,the strain stress (small) behavior of a rubber using fringe projection technique is performed.

The paper is divided in five chapters. The first chapter deals with the general background of moiré patterns and the working principle of diffraction gratings. The second chapter is about moiré interference and detail mathematical methods of calculating fringe spacing.
The third chapter tells about deformation and its measurement. It includes strain stress analysis of materials,in general,and elastomers,in particular. The fourth chapter is about experimental techniques and materials used. The fifth chapter is results and discussion of the experiment.

Chapter 1

Moiré Patterns and Diffraction Grating

1.1 Moiré Patterns

1.1.1 General Background

The fringes with which this report is concerned were observed as long ago as 1874 by Lord Rayleigh. In a paper 'on the manufacture and theory of diffraction gratings'[1], he wrote: "if two photographic copies (of diffraction gratings) containing the same number of lines to the inch be placed in contact, film to film,in such a way that the lines are nearly parallel in the two gratings, a system of parallel bars develops itself,whose direction bisects the external angle between the directions of the original lines and whose distance increases as the angle of inclination diminishes...."

The 'parallel bars' described in this extract are now commonly called moiré fringes, a name probably suggested by the fact that when observed without special apparatus by merely looking through the crossed gratings at a bright wall(window), they appear very faint. In physics, a moiré pattern is an interference pattern created, for example, when two grids are overlaid at an angle, or when they have slightly different mesh sizes. The term "moiré",in optics refers to a beat pattern produced between two gratings of approximately equal spacing. In all circumstances in which moiré fringes are observed, they are, in fact, interference fringes produced by the slightly divergent wave fronts of beams which,though differently treated by each of the two gratings,

emerge in every nearly the same direction from the second one. The interference effects therefore account completely for the fringes produced by gratings in completely coherent illumination.

Although the normal circumstances in which moiré fringes are produced are those described by Rayleigh-two transparent gratings of practically the same pitch mounted face to face with their surfaces in contact, or at least very close, they are also produced if the pitches are in the ratio of two small integers, for example 2:1,3:1,3:2. Fringes may also be observed in various other cases. They may be produced by projecting an image of one grating on the surface of another, in which case gratings of any relative pitches may be used, equality of pitch of the second grating with that of the image of the first being obtained by adjusting the magnification.

1.2 Fundamental Considerations of a diffraction Grating

A diffraction grating is an optical component with a regular pattern, which splits (diffracts) light into several beams traveling in different directions. It generally consists of a plastic replica of a glass or metal surface on which a large number of fine, parallel, evenly spaced lines have been ruled [3]. The directions of the diffracted beams depend on the spacing of the grating and the wavelength of the light so that the grating acts as a dispersive element. For the understanding of moiré phenomena, it is necessary to take account of some of the essential properties of a diffraction grating.

The ruled area of a grating, if examined with a microscope of suitable resolving power,appears to consist of straight parallel strips of equal width,having some characteristic features which form a pattern that is exactly repeated in each strip. The width of these strips is variously referred to as the grating space or pitch or ruling width. The pitch is often specified by its reciprocal, the number of rulings per unit length. It is a common practice in this connexion to refer to the rulings as lines,as,for instance, when a grating is said to have 600 lines per millimeter.

Lines in different strips which are similarly situated between the boundaries of the strip in which they occur will be termed corresponding lines. At points anywhere

on the members of any set of corresponding lines, the local effect of the grating on disturbances passing through it is the same.

1.2.1 Working Principle of a Diffraction Grating

A diffraction grating can be thought of as a collection of narrow slits. Multiple slit interference can then be used to model the effects of a grating on incident light. Light of a single wavelength passing through the grating (or reflected from the grating) is diffracted by the grooves; in most directions the light diffracted from one groove cancels from that diffracted from other grooves through destructive interference. In a certain finite number of directions, though, all of the rays from the grooves interfere constructively. Such directions correspond to diffraction orders. Many orders exist when the wavelength of the light diffracted is much smaller than the distance between adjacent grooves; few order exists when this wavelength is comparable to the groove spacing, and no orders exists except the reflected ray when the wavelength exceeds two times the groove spacing (in the last case the grating behaves as a mirror).

1.2.2 The basis of grating action

The characteristic behavior of a diffraction grating is due to phase changes,amplitude changes, or both, suffered by disturbances passing through it. These changes varying from point to point across each ruling in a pattern which is the same everywhere along each ruling and is exactly repeated in every ruling.

In the majority of gratings, the amplitude variation is practically zero.The action of these gratings depends almost entirely on the variation of the phase changes suffered by the disturbances at different points of each ruling on account of the differences in optical path.

The one feature common to all gratings is that the effect produced through disturbance, at corresponding points of every ruling is the same. The result of this,as fundamental investigations show, is that the transmitted energy can only travel out from the grating in a limited number of directions. These are directions such that the distance, measured along the incident and emergent rays, from a wavefront of the incident beam to a wavefront in one of the emergent beams is constant for all rays incident at points of the grating surface. This distance is either the same at all

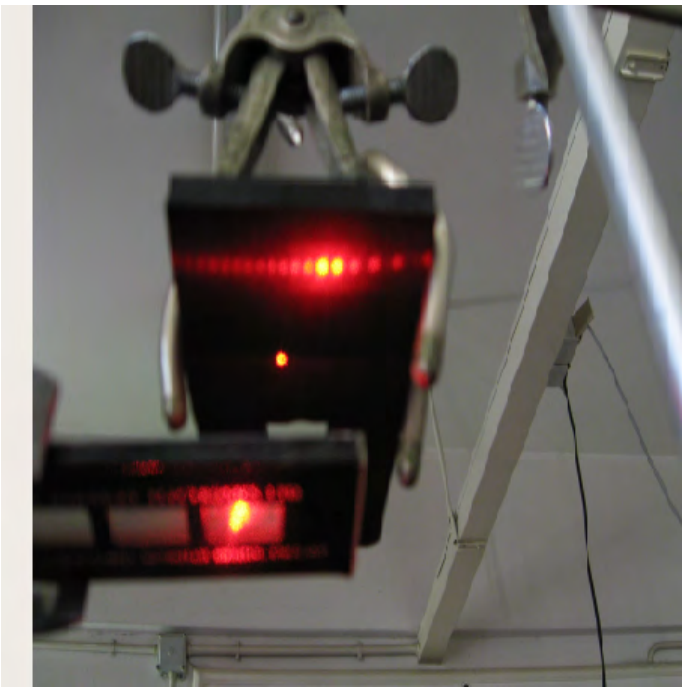

Figure 1.1: Diffraction gratings in action

other points or differs by one, two, three or more wavelengths for rays incident at corresponding points of successive rulings. In any direction other than these, there is destructive interference between some members of the set and if the number of rulings is very large, this interference is complete and no energy will transmit.

In general, a grating affects the elementary disturbances passing through it by imposing changes of phase and amplitude whose amounts at any point of the grating surface are functions of position of the point within a ruling. We may refer to these functions as the phase or amplitude functions of a grating.

1.2.3 Phase and amplitude functions

In this regard, phase or amplitude functions don't refer to the actual phase or amplitude of the disturbances at the grating surface but to the changes imposed, in passing

through the grating, on the phases and amplitudes of the incident disturbances.

Phase or amplitude functions may be of simple type; linear or sinusoidal variations, for example, being among those sought by designers. There is no general formula for the change of phase or amplitude imposed on the disturbance transmitted at any given point. It would seem , therefore,that although the essential physical properties of any grating are comprised in these functions,no quantitative proposition of universal validity can be made about them.

Chapter 2

Moiré Interferometry and Fringe Spacing

2.1 Moiré Interference

Moiré fringes can be thought as a superposition of two plane waves which keeps an angle between their traveling directions. In the regions where the waves are on phase, a constructive interference is generated,showing clear patterns and in the case of destructive interference, dark patterns are formed.

Moiré is a useful technique for aiding in the understanding of interferometry. Fig.2.1 below shows the moiré pattern (beat pattern) produced by two identical straight line gratings rotated by a small angle relative to each other. A dark fringe is produced where the dark lines are out of step one-half period, and a bright fringe is produced where the dark lines for one grating fall on top of the corresponding dark lines for the second grating. If the angle between the two gratings is increased,the separation between the bright and dark fringes decreases. If the gratings are not identical straight-line gratings,the moiré pattern (bright and dark fringes) will not be straight equi-spaced fringes.

2.2 Fringe Spacing Determination

Let the intensity transmission function for two arbitrary gratings $f_1(x;y)$ and $f_2(x;y)$ be given by [10]:

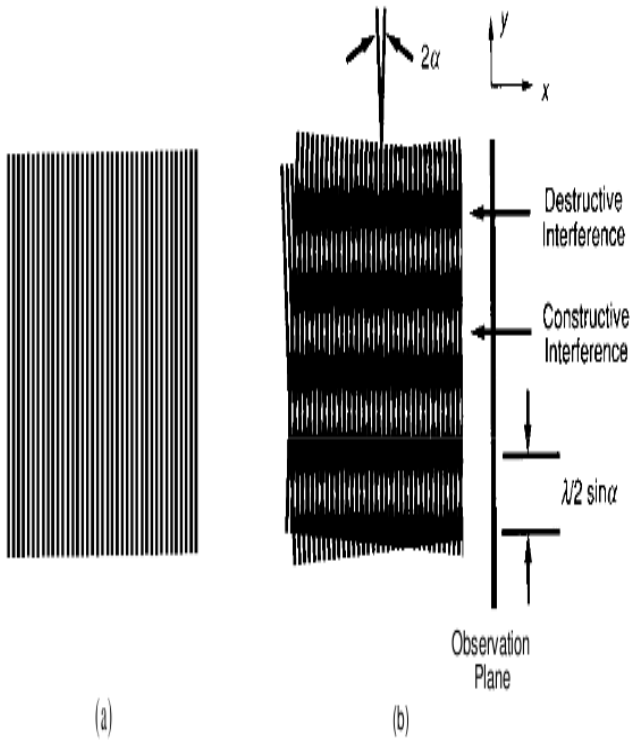

Figure 2.1: (a)Straight Line Grating (b)Moiré between two straight line gratings of the same pitch at an angle α with respect to each other

$$f_1(x,y) = a_1 + \sum_{n=1}^{\infty} b_{1n} cos[n\phi_1(x,y)] \quad (2.2.1)$$

$$f_2(x,y) = a_2 + \sum_{m=1}^{\infty} b_{2m} cos[m\phi_2(x,y)] \quad (2.2.2)$$

where $\phi(x,y)$ is the function describing the basic shape of the grating lines.
where

$$\phi(x,y) = 2\Pi n \quad (2.2.3)$$

(at the center of each bright line)

$$\phi(x,y) = 2\Pi(n + \frac{1}{2}) \quad (2.2.4)$$

(at the center of each dark line)
The b coefficients determine the profile of the grating lines (i.e square,sinusoidal wave...). When these two gratings are superimposed, the resulting intensity transmission function is given by:

$$f_1(x,y)f_2(x,y) = a_1a_2 + a_1 \sum_{n=1}^{\infty} b_{2m} cos[m\phi_2(x,y)] + a_2 \sum_{n=1}^{\infty} b_{1n} cos[n\phi_1(x,y)] \quad (2.2.5)$$

$+ \sum_{m=1}^{\infty} \sum_{n=1}^{\infty} b_{1n}b_{2m} cos[n\phi_1(x,y)]cos[m\phi_2(x,y)]$
The first three terms of equation 2.2.5 provide information that can be determined by looking at the two patterns separately. The last term is the interesting one and can be written as:

$$P = \sum_{m=1}^{\infty} \sum_{n=1}^{\infty} b_{1n}b_{2m} cos[n\phi_1(x,y)]cos[m\phi_2(x,y)] \quad (2.2.6)$$

But
$cos[n\phi_1(x,y)]cos[m\phi_2(x,y)] = \frac{1}{2}cos[n\phi_1(x,y) - m\phi_2(x,y)] + \frac{1}{2}cos[n\phi_1(x,y) + m\phi_2(x,y)]$
Thus

$$P = \frac{1}{2}b_{11}b_{21}cos[\phi_1(x,y) - \phi_2(x,y)] + \frac{1}{2} \sum_{m=1}^{\infty} \sum_{n=1}^{\infty} b_{1n}b_{2m} cos[n\phi_1(x,y) \quad (2.2.7)$$

$-m\phi_2(x,y)]$; n and m both $\neq 1 + \frac{1}{2}\sum_{m=1}^{\infty}\sum_{n=1}^{\infty} b_{1n}b_{2m}cos[n\phi_1(x,y) + m\phi_2(x,y)]$
This implies that when two gratings are superimposed, the sum and difference between the two gratings can be obtained. The first term of equation 2.2.7 represents the difference between the fundamental pattern masking up the two gratings. It can be used to predict the moiré pattern shown in Fig 2.1. Assuming that two gratings are oriented with an angle 2α between them with the Y-axis of the coordinate system bisecting this angle, the two grating functions $\Phi_1(x,y)$ and $\Phi_2(x,y)$ can be written as:

$$\Phi_1(x,y) = \frac{2\pi(xcos\alpha + ysin\alpha)}{\lambda_1} \tag{2.2.8}$$

$$\Phi_2(x,y) = \frac{2\pi(xcos\alpha - ysin\alpha)}{\lambda_2} \tag{2.2.9}$$

where λ_1 and λ_2 are the line spacings of the two gratings. Rewriting the above equations yield:

$$\Phi_1(x,y) - \Phi_2(x,y) = \frac{2\pi xcos\alpha}{\lambda_{beat}} + \frac{4\pi ysin\alpha}{\lambda_{av}} \tag{2.2.10}$$

where λ_{av} is the average line spacing, and λ_{beat} is the beat wavelength between the two gratings. And

$$\lambda_{beat} = \frac{\lambda_1\lambda_2}{\lambda_2 - \lambda_1} \tag{2.2.11}$$

$$\lambda_{av} = \frac{2\lambda_1\lambda_2}{\lambda_1 + \lambda_2} \tag{2.2.12}$$

Using equation 2.2.7, the moiré or beat will be lines whose centers satisfy the equation :

$$\Phi_1(x,y) - \Phi_2(x,y) = M2\pi \tag{2.2.13}$$

Now, we can consider three separate cases for moiré fringes.

Case1: When $\lambda_1 = \lambda_2 = \lambda$

In this case, the first term of equation 2.2.10 is zero, and the fringe centers are given

by:

$$M\lambda = 2ysin\alpha \tag{2.2.14}$$

Where M is an integer corresponding to the fringe order. Equation 2.2.14 is the equation of equi-spaced horizontal lines as seen in fig.2.2.

Case2: When the gratings are parallel to each other with $\alpha = 0$
In this case, the second term of equation 2.2.10 will vanish. The moiré will then be lines that satisfy:

$$M\lambda_{beat} = x \tag{2.2.15}$$

These fringes are equally spaced, vertical lines parallel to the Y-axis.

Case3:When the two gratings have different line spacings and the angle between the gratings is non-zero.
For this case, the equation of the moiré fringes will be:

$$M\lambda_{av} = \frac{\lambda_{av} x cos\alpha}{\lambda_{beat}} + 2ysin\alpha \tag{2.2.16}$$

This is the equation of straight lines whose spacing and orientation is dependent on the relative difference between the two grating spacings and the angle between the gratings. Fig 2.2 shows moiré patterns for these three cases.

The orientation and spacing of the moire fringes for the general case (case 3) can be determined from the geometry shown in Fig.2.3.

The distance AB can be written in terms of the two grating spacings:

$$AB = \frac{\lambda_1}{sin(\theta - \alpha)} = \frac{\lambda_2}{sin(\theta + \alpha)} \tag{2.2.17}$$

Where θ is the angle the moiré fringes make with the y-axis. After rearranging the fringe orientation angle θ is given by:

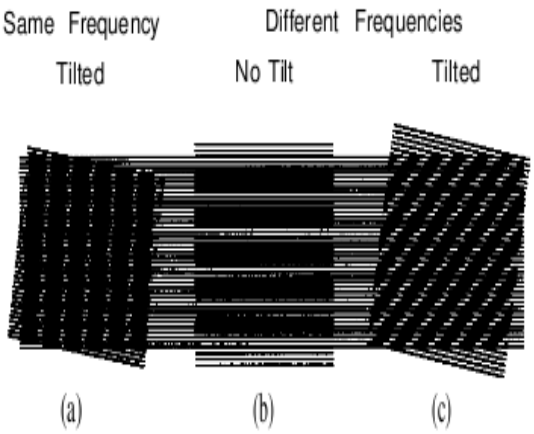

Figure 2.2: Moiré patterns caused by two straight-line gratings

$$tan(\theta) \quad = \quad tan(\alpha)\frac{\lambda_1 + \lambda_2}{\lambda_2 - \lambda_1} \tag{2.2.18}$$

When $\alpha = 0$ and $\lambda_1 \neq \lambda_2$,$\theta = 0$ and when $\lambda_1 = \lambda_2$ with $\alpha \neq 0$,$\theta = 90^0$ as expected. The fringe spacing perpendicular to the fringe lines can be found by equating quantities for the distance DE.

$$DE \quad = \quad \frac{\lambda_1}{sin(2\alpha)} = \frac{C}{sin(\theta + \alpha)} \tag{2.2.19}$$

Where C is the fringe spacing or contour interval. This can be rearranged as:

$$C = \lambda_1[\frac{sin(\theta + \alpha)}{sin2\alpha}] \tag{2.2.20}$$

By substituting for the fringe orientation θ, the fringe spacing can be found interms of the grating spacings and angle between the gratings:

$$C = \frac{\lambda_1\lambda_2}{\sqrt{\lambda_2^2 sin^2 2\alpha + (\lambda_2 cos2\alpha - \lambda_1)^2}} \tag{2.2.21}$$

In the limit that $\alpha = 0$ and $\lambda_1 \neq \lambda_2$,the fringe spacing equals λ_{beat},and in the limit that $\lambda_1 = \lambda_2 = \lambda$ and $\alpha \neq 0$,the fringe spacing equals $\frac{\lambda}{2\sin\alpha}$.

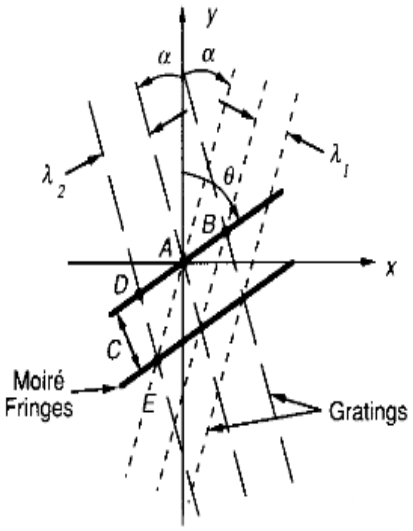

Figure 2.3: Geometry used to determine spacing and angle of moiré fringes between two gratings of different frequencies tilted with respect to one another.

The single grating shown in Fig.2.1 can be thought as a plane wave traveling to the right, where the distance between the grating lines is equal to the wavelength of light. Superimposing the two sets of grating lines can be taken as superimposing two plane waves with an angle of 2α between their direction of propagation. Where the two waves are in phase, bright fringes result and where they are out of phase dark fringes result. The spacing of the interference fringes is given by $C = \frac{\lambda}{2\sin\alpha}$ where λ is now the wavelength of light.

2.3 Fringe Projection

A simple approach for contouring is to project interference fringes or a grating onto an object and then view from another direction. Fig.2.4 shows the optical setup for this measurement. Assuming a collimated illumination beam and viewing the fringes with a telecentric optical system,straight equally spaced fringes are incident on the object, producing equally spaced contour intervals. The departure of a viewed fringe from a straight line shows the departure of the surface from a plane reference surface.

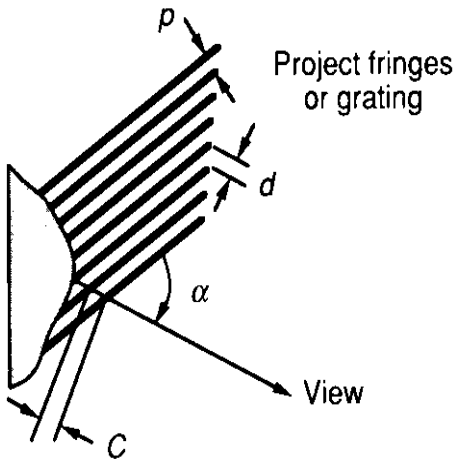

Figure 2.4: Projection of fringes or grating onto object and viewed at an angle α. p is the grating pitch or fringe spacing and C is the contour interval.

When the fringes are viewed at an angle α relative to the projection direction, the spacing of the lines perpendicular to the viewing direction will be:

$$d = \frac{p}{cos\alpha} \tag{2.3.1}$$

The contour interval C (the height between adjacent contour lines in the viewing direction) is determined by the line or fringe spacing projected onto the surface and the angle between the projection and viewing directions:

$$C = \frac{p}{sin\alpha} = \frac{d}{tan\alpha} \tag{2.3.2}$$

These contour lines are planes of equal height, and the sensitivity of the measurement is determined by α. The larger the angle α, the smaller the contour interval. If $\alpha = 90^o$, then the contour interval is equal top,and the sensitivity is a maximum. The reference plane will be parallel to the direction of the fringes and perpendicular to the viewing direction. Eventhough the maximum sensitivity can be obtained at 90^o, this angle between the projection and viewing directions will produce a lot of

unacceptable shadows on the object. These shadows will lead to areas with missing data where the object cannot be contoured. When $\alpha = 0$, the contour interval is infinite, and the measurement sensitivity is zero. To provide the best results, an angle no larger than the largest slope on the surface should be chosen.

2.4 Shadow Moiré

A simple method of moiré interferometry for contouring objects uses a single grating placed in front of the object as shown in Fig.2.5. The grating in front of the object produces a shadow on the object that is viewed from a different direction through the grating. A low frequency beat or moiré pattern is seen.

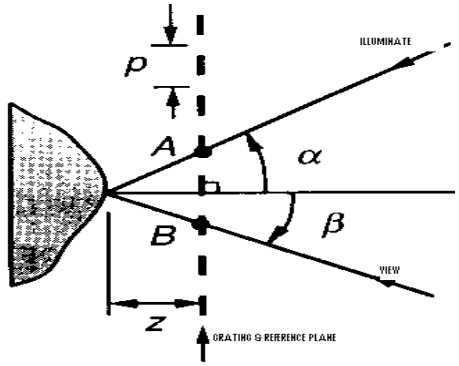

Figure 2.5: Geometry for shadow moiré with illumination and viewing at infinity, i.e., parallel illumination and viewing

This pattern is due to the interference between the grating shadows on the object and the grating as viewed. Assuming that the illumination is collimated and that the object is viewed at infinity or through a telecentric optical system,the height z between the grating and the object point can be determined from the geometry shown in Fig.2.6 (Meadows et al.1970;Takasaki 1973;Chiang 1983).

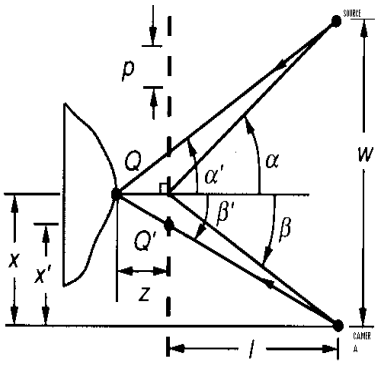

Figure 2.6: Geometry for shadow moiré with illumination and viewing at finite distances.

This height is given by:

$$z = \frac{Np}{tan\alpha + tan\beta} \tag{2.4.1}$$

Where α is the illumination angle, β is the viewing angle, p is the spacing of the grating lines, and N is the number of grating lines between the points A and B. The contour interval in a direction perpendicular to the grating will simply be given by:

$$C = \frac{p}{tan\alpha + tan\beta} \tag{2.4.2}$$

Again, the distance between the moiré fringes in the beat pattern depends on the angle between the illumination and viewing directions. The larger the angle,the smaller the contour interval.If the high frequencies due to the original grating are filtered out, then only the moiré interference term is seen.The reference plane will be parallel to the grating. The contour interval for shadow moiré is the same as that calculated for projected fringe contouring,when one of the angles is zero with d=p.

Most of the time, it is difficult to illuminate an entire object with a collimated beam. Therefore, it is important to consider the case of finite illumination and viewing distances. It is possible to derive this for a very general case (Meadows et al.1970;Takasaki 1970;Bell 1985); however, for simplicity, only the case where the illumination and viewing positions are the same distance from the grating will be considered. Fig.2.6

shows a geometry where the distance between the illumination source and the viewing camera is given by w, and the distance between these and the grating is L. The grating is assumed to be close enough to the object surface so that diffraction effects are negligible.

In this case the height between the object and the grating is given by:

$$z = \frac{Np}{tan\alpha' + tan\beta'} \tag{2.4.3}$$

Where α' and β' are the illumination and viewing angles at the object surface. These angles change for every point on the surface and are different from α and β in Fig.2.6, where α and β are the illumination and viewing angles at the grating (reference) surface. The surface height can also be written as:

$$z = NC(z) = \frac{NpL}{w - Np} \tag{2.4.4}$$

This equation indicates that the height is a complex function depending on the position of each object point. Thus, the distance between contour intervals is dependent on the height of the surface and the number of fringes between the grating and the object.

2.5 Applications of moiré techniques

Since Lord Rayleigh first noticed the phenomena,moiré techniques have been used for a number of testing applications. Righi (1887) first noticed that the relative displacement of two gratings could be determined by observing the movement of the moiré fringes. The next significant advance in the use of moiré was presented by Weller and Shepherd (1948). They used moiré to measure the deformation of an object under applied stress-by looking at the differences in a grating pattern before and after the applied stress. They were also the first to use shadow moiré, where a grating is placed in front of a non flat surface to determine the shape of the object behind it by using the shape of the moiré fringes.

Moreover, projection moiré techniques can also be used for optical gauging and deformation measurement. Meadows et al(1970) also reported some of the uses of moiré to measure surface topography. These techniques could be applied applied for determination of, for instance, wood specimens using isostrain patterns generated [4];for computer based topography and interferometry analysis; for micro scale flow visualization [7];for measurement of thermally induced warpage package [5] and the like. Moiré has also been used to compare an object to a master and for vibration analysis(Der Hovanesian and Yung 1971;Gasvik 1987).

Chapter 3

Deformation

3.1 Definition

In continuum mechanics, deformation is the change in shape or size of a continuum body after it undergoes a displacement between an initial or undeformed configuration ,$k_0(b)$ at time t_0, and a current or deformed configuration , $k_t(b)$ at the current time,t .

In general, the displacement of a continuum body has two components: a rigid-body displacement component and a deformation component. If after a displacement of the continuum there is a relative displacement between particles, a deformation has occurred. On the other hand, if after displacement of the continuum the relative displacement between particles in the current configuration is zero i.e. the distance between particles remains unchanged, then there is no deformation and a rigid-body displacement is said to have occurred.

Deformation results from stresses within the continuum induced by external forces or due to changes in its temperature. The relation between stresses and induced strains is expressed by constitutive equations, e.g. Hooke's law for linear elastic materials. Deformations which are recovered after the external forces have been removed, are called elastic deformations. In this case, the continuum completely recovers its original configuration. On the other hand, irreversible deformations, which remain even after external forces have been removed, are called plastic deformations. Such deformations occur in material bodies after stresses have surpassed a certain threshold value known as the elastic limit or yield stress, and are the result of slip, or dislocation mechanisms at the atomic level. Deformation is measured in units of length.

3.2 Strain

Strain is the geometrical measure of deformation representing the relative displacement between particles in the material body, i.e. a measure of how much a given displacement differs locally from a rigid-body displacement (Jacob Lubliner). Strain defines the amount of stretch or compression along a material line elements or fibers, i.e. normal strain, and the amount of distortion associated with the sliding of plane layers over each other, i.e. shear strain, within a deforming body (David Rees). Strain is a dimensionless quantity, which can be expressed as a decimal fraction or a percentage.

The state of strain at a material point of a continuum body is defined as the totality of all the changes in length of material lines or fibers, i.e. normal strain, which pass through that point and also the totality of all the changes in the angle between pairs of lines initially perpendicular to each other, i.e. shear strain, radiating from this point. However, it is sufficient to know the normal and shear components of strain on a set of three mutually perpendicular directions. If there is an increase in length of the material line, the normal strain is called tensile strain, otherwise, if there is reduction or compression in the length of the material line, it is called compressive strain.

3.2.1 Strain measurement

Depending on the amount of strain, i.e. local deformation, the analysis of deformation is subdivided into three deformation theories:

1.Finite strain theory, also called large strain theory, deals with deformations in which both rotations and strains are arbitrarily large. In this case, the undeformed and deformed configurations of the continuum are significantly different and a clear distinction has to be made between them. This is commonly the case with elastomers, plastically-deforming materials and other fluids and biological soft tissue.

2.Infinitesimal strain theory, also called small strain theory, where strains and rotations are both small. In this case, the undeformed and deformed configurations of the body can be assumed identical. The infinitesimal strain theory is used in the analysis

of deformations of materials exhibiting elastic behavior, such as materials found in mechanical and civil engineering applications, e.g. concrete and steel.

3.Large-displacement or large-rotation theory, which assumes small strains but large rotations and displacements.

In each of these theories the strain is then defined differently. The engineering strain is the most common definition applied to materials used in mechanical and structural engineering, which are subjected to very small deformations.

The Cauchy strain or engineering strain is expressed as the ratio of total deformation to the initial dimension of the material body in which the forces are being applied [20]. The engineering normal strain or engineering extensional strain of a material line element or fiber axially loaded is expressed as the change in length per unit of the original length of the line element or fibers. The normal strain is positive if the material fibers are stretched or negative if they are compressed. Thus, we have

$$e = \frac{\Delta L}{L} = \frac{l - L}{L} \tag{3.2.1}$$

where l is the final length of the fiber.

The engineering shear strain is defined as the change in the angle between two material line elements initially perpendicular to each other in the undeformed or initial configuration. The stretch ratio or extension ratio is a measure of the extensional or normal strain of a differential line element, which can be defined at either the undeformed configuration or the deformed configuration. It is defined as the ratio between the final length, l, and the initial length,L, of the material line.

$$\lambda = \frac{l}{L} \tag{3.2.2}$$

The extension ratio is related to the engineering strain by

$$e = \frac{l - L}{L} = \lambda - 1 \tag{3.2.3}$$

This equation implies that the normal strain is zero, i.e. no deformation, when the stretch is equal to unity. The stretch ratio is used in the analysis of materials that

exhibit large deformations, such as elastomers, which can sustain stretch ratios of 3 or 4 before they fail. The logarithmic strain ,ε, also called natural strain, or true strain, by considering an incremental strain (Ludwik),$\delta\varepsilon$, is given by:

$$\delta\varepsilon = \frac{\delta l}{l} \tag{3.2.4}$$

The logarithmic strain is obtained by integrating this incremental strain:

$$\int \delta\varepsilon = \int_L^l \frac{\delta l}{l} \tag{3.2.5}$$

$$\varepsilon = ln(\frac{l}{L}) = ln\lambda \tag{3.2.6}$$

Or

$$\varepsilon = ln(1+e) = e - e^2 + e^3 - .... \tag{3.2.7}$$

Where e is the engineering strain. The logarithmic strain provides the correct measure of the final strain when deformation takes place in a series of increments, taking into account the influence of the strain path.

3.3 Description of Deformation

It is convenient to identify a reference configuration or initial geometric state of the continuum body which all subsequent configurations are referenced from. The reference configuration need not to be one the body actually will ever occupy. Often, the configuration at t=0 is considered the reference configuration,$k_0(B)$. The configuration at the current time t is the current configuration.

For deformation analysis, the reference configuration is identified as undeformed configuration, and the current configuration as deformed configuration. Additionally,

time is not considered when analyzing deformation, thus the sequence of configurations between the undeformed and deformed configurations are of no interest.

There is continuity during deformation of a continuum body in the sense that:
1.The material points forming a closed curve at any instant will always form a closed curve at any subsequent time.
2.The material points forming a closed surface at any instant will always form a closed surface at any subsequent time and the matter within the closed surface will always remain within.

3.3.1 Displacement

A change in the configuration of a continuum body results in a displacement. The displacement of a body has two components: a rigid-body displacement and a deformation. A rigid-body displacement consist of a simultaneous translation and rotation of the body without changing its shape or size. Deformation implies the change in shape and/or size of the body from an initial or undeformed configuration $k_0(B)$ to a current or deformed configuration $k_t(B)$.

If after a displacement of the continuum there is a relative displacement between particles, a deformation has occurred. On the other hand, if after displacement of the continuum the relative displacement between particles in the current configuration is zero i.e. the distance between particles remains unchanged, then there is no deformation and a rigid-body displacement is said to have occurred.

3.3.2 Stress Strain curve

During testing of a material sample, the stress strain curve is a graphical representation of the relationship between stress, derived from measuring the load applied on the sample, and strain, derived from measuring the deformation of the sample, i.e. elongation, compression, or distortion. The nature of the curve varies from material to material.
The following diagrams illustrate the stress strain behavior of typical materials in terms of the engineering stress and engineering strain where the stress and strain are calculated based on the original dimensions of the sample and not the instantaneous

values.

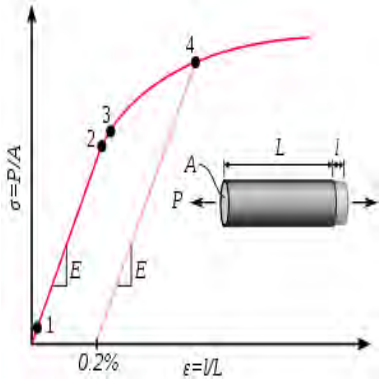

Figure 3.1: Ductile Materials

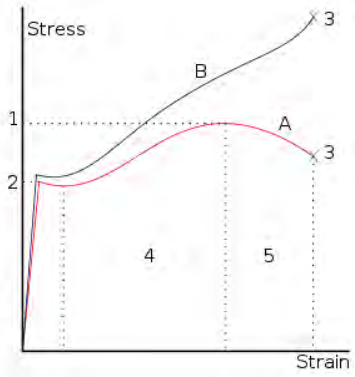

Figure 3.2: A stress strain curve typical of structural steel

1. Ultimate Strength 2. Yield Strength 3. Rupture 4. Strain hardening region 5. Necking region.
A: Apparent stress (F/A_0)
B: Actual stress (F/A)
Steel generally exhibits a very linear stress strain relationship up to a well defined yield point (fig 3.2). The linear portion of the curve is the elastic region and the slope is the modulus of elasticity or Young's Modulus. After the yield point, the curve typically decreases slightly. As deformation continues, the stress increases on account of strain hardening until it reaches the ultimate strength. Until this point, the cross-sectional area decreases uniformly because of contractions.

However, beyond this point a neck forms where the local cross-sectional area decreases more quickly than the rest of the sample resulting in an increase in the true stress. Conversely, if the curve is plotted in terms of true stress and true strain, the stress will continue to rise until failure. Eventually the neck becomes unstable and the specimen ruptures (fractures). Less ductile materials such as aluminum and medium to high carbon steels do not have a well defined yield point. For these materials the yield strength is typically determined by the offset yield method, by which a line is drawn parallel to the linear elastic portion of the curve and intersecting the abscissa at some arbitrary value,most commonly 0.2 percent. The intersection of this line and the stress strain curve is reported as the yield point.

Brittle materials such as concrete and carbon fiber do not have a yield point, and

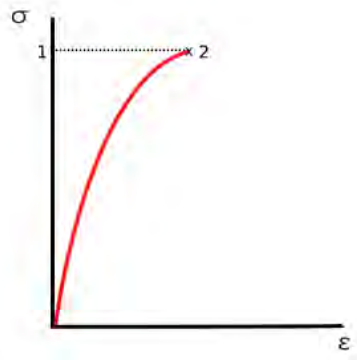

Figure 3.3: Stress Strain curve for Brittle Materials

do not strain harden which means that the ultimate strength and breaking strength

are the same. A most unusual stress strain curve is shown in fig 3.3. Typical brittle materials like glass do not show any plastic deformation but fail while the deformation is elastic. One of the characteristics of a brittle failure is that the two broken parts can be reassembled to produce the same shape as the original component as there will not be a neck formation like in the case of ductile materials. A typical stress strain curve for a brittle material will be linear.

3.3.3 Stress Strain relations

Elasticity is the ability of a material to return to its previous shape after stress is released. In many materials, the relation between applied stress and the resulting strain is directly proportional (up to a certain limit), and a graph representing those two quantities is a straight line. The slope of this line is known as Young's Modulus, or the "Modulus of Elasticity". The Modulus of Elasticity can be used to determine stress strain relationships in the linear-elastic portion of the stress-strain curve. The linear-elastic region is taken to be between 0 and 0.2 percent strain, and is defined as the region of strain in which no yielding (permanent deformation) occurs.

Plasticity or plastic deformation is the opposite of elastic deformation and is accepted as unrecoverable strain. Plastic deformation is retained even after the relaxation of the applied stress. Most materials in the linear-elastic category are usually capable of plastic deformation. Brittle materials, like ceramics, do not experience any plastic deformation and will fracture under relatively low stress. Materials such as metals usually experience a small amount of plastic deformation before failure while soft or ductile polymers will plastically deform much more.

3.4 Strain Energy

The area under the stress strain curve up to a given value of strain is the total mechanical energy per unit volume consumed by the material in straining it to that value. This is given by:
$U = \int_0^L \frac{FdL}{A_0 L_0} = \int_0^\epsilon \sigma d\epsilon$
In the absence of molecular slip and other mechanisms for energy dissipation, this mechanical energy is stored reversibly within the material as strain energy. When the stresses are low enough that the material remains in the elastic range, the strain

energy is just the triangular area in Fig 3.4 below.

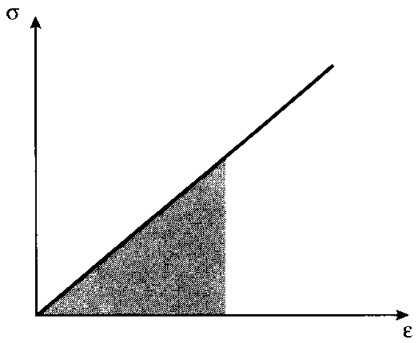

Figure 3.4: Strain Energy = Area under stress-strain curve

The area up to the yield point is termed as the *modulus of resilience*, and the total area up to fracture is termed the *modulus of toughness*[15]; as shown in Fig 3.5. The term 'resilience'alludes to the concept that up to the point of yielding, the material is unaffected by the applied stress and upon unloading will return to its original shape. The modulus of resilience is then the quantity of energy the material can absorb without suffering damage. Similarly, the modulus of toughness is the energy needed to completely fracture the material. Materials showing good impact resistance are generally those with high moduli of toughness.

3.5 Strength of Materials

In materials science, the strength of a material refers to the material's ability to withstand an applied stress without failure. Yield strength refers to the point on the engineering stress-strain curve (as opposed to true stress-strain curve) beyond which the material begins deformation that cannot be reversed upon removal of the loading. Ultimate strength refers to the point on the engineering stress-strain curve corresponding to the maximum stress. The applied stress may be tensile, compressive, or shear.

A material's strength is dependent on its microstructure. The engineering processes

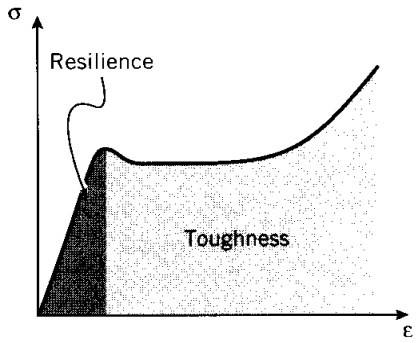

Figure 3.5: Moduli of resilience and toughness

to which a material is subjected can alter this microstructure. In general, the yield strength of a material is an adequate indicator of the material's mechanical strength. Considered in tandem with the fact that the yield strength is the parameter that predicts plastic deformation in the material, one can make informed decisions on how to increase the strength of a material depending its microstructural properties and the desired end effect. Strength is considered in terms of compressive strength, tensile strength, and shear strength, namely the limit states of compressive stress, tensile stress and shear stress, respectively. The effects of dynamic loading is probably the most important practical part of the strength of materials, especially the problem of fatigue. Repeated loading often initiates brittle cracks, which grow slowly until failure occurs.

However, the term strength of materials most often refers to various methods of calculating stresses in structural members. The methods that can be employed to predict the response of a structure under loading and its susceptibility to various failure modes may take into account various properties of the materials other than material (yield or ultimate) strength.

Uniaxial stress is expressed by $\sigma = \frac{F}{A}$ where F is the force [N] acting on an area A [m^2]. The area can be the undeformed area or the deformed area, depending on whether engineering stress or true stress is used.

Compressive stress (or compression) is the stress state caused by an applied load that acts to reduce the length of the material (compression member) in the axis of the applied load, in other words the stress state caused by squeezing the material.

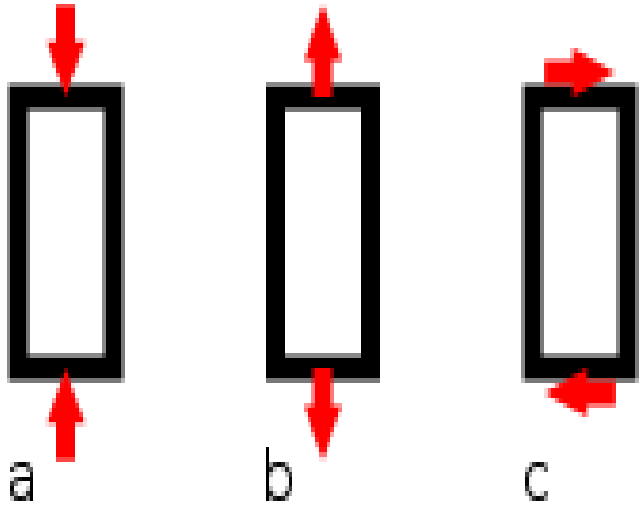

Figure 3.6: A material being loaded in a) compression, b) tension, c) shear.

A simple case of compression is the uniaxial compression induced by the action of opposite, pushing forces. Compressive strength for materials is generally higher than that of tensile stress. Tensile stress is the stress state caused by an applied load that tends to elongate the material in the axis of the applied load, in other words the stress caused by pulling the material. The strength of structures of equal cross sectional area loaded in tension is independent of cross section geometry. Materials loaded in tension are susceptible to stress concentrations such as material defects or abrupt changes in geometry. However, materials exhibiting ductile behavior (metals for example) can tolerate some defects while brittle materials (such as ceramics) can fail well below their ultimate stress.

Shear stress is the stress state caused by opposing forces acting along parallel lines of action through the material, in other words the stress caused by sliding faces of the material relative to one another.

Yield strength is the lowest stress that gives permanent deformation in a material. In some materials, like aluminium alloys, the point of yielding is hard to define, thus it is usually given as the stress required to cause 0.2 percent plastic strain.

Compressive strength is a limit state of compressive stress that leads to compressive failure in the manner of ductile failure (infinite theoretical yield) or in the manner of brittle failure (rupture as the result of crack propagation), or sliding along a weak plane.

3.6 Elastomers Stress-Strain Behavior

Elastomers are materials of a very high molecular weight, generally composed of one or more monomers polymerised or co-polymerised together to form a polymer (or copolymer). The different distinct categories of the stress strain behavior of elastomers make engineering design with these materials so challenging. They exhibit large deformation response and non linearity of the stress strain curve. A rubber test piece changes its stress strain curve radically after the first application of load and continue to change behavior thereafter, depending primarily on the magnitude and timing of the deformations [11]. We will refer to this category of behaviors as cyclic or time dependent properties. The second category is the large deformation response. This important behavior is seen in elastomer's soft or low modulus response to applied loads or deformations. Commonly, it is the principal reason or selecting an elastomer for a particular part or component. Non linear stress strain response is the third category of behaviors which challenges the design engineer. On the other hand foams behave similar to ductile materials with apparent yield points,high elongation and relatively high ultimate strengths in compressive stress strain tests [16].

3.6.1 Characteristics of Stress-Strain Behavior

After considering the huge percent deformation, elastomer's most obvious feature is its non linearity. Note that there is no constant value of the elastic modulus, i.e., $\delta = Ee$ is only true if E is a variable. It is this characteristic that limits the usefulness of simple design equations which depend on linear behavior. But at small strain values, some writers refer to the knee of the curve ($1.0 < \lambda < 1.5$) as a yield point.A typical elastomer can extend to 300 percent strain without rupture. The difference in stress ,$\Delta\delta$, is named hysteresis. Hysteresis is caused by internal friction, which resists both extension and contraction. Hysteresis varies with the elastomer; it is least in unreinforced natural rubber and larger in most other elastomers. It increases with the amount of reinforcing material present and with the strain rate of the test.

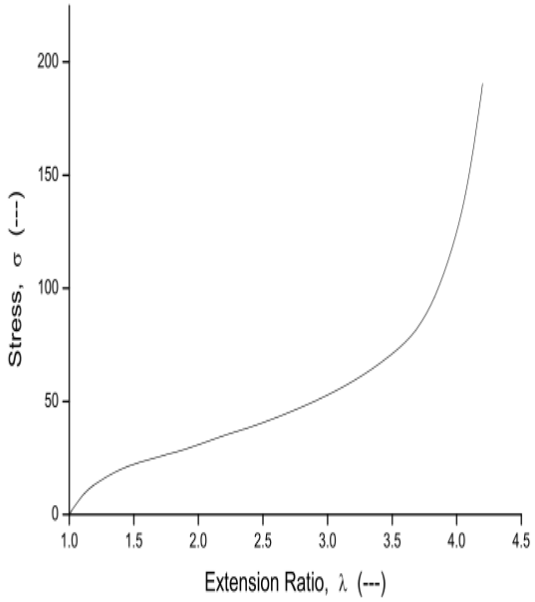

Figure 3.7: large deformation behavior of an elastomer.

Chapter 4

Experimental Technique

4.1 Apparatus and Material

To see the moiré fringes and do the strain stress analysis, the following materials were used.

- He-Ne laser source with power 1mw,wavelength 632.8nm.
- Two straight line diffraction gratings with 100lines/mm and 300 lines/mm pitches.
- Micrometer;beam-balance,Stands and clips.
- Lenses with 50mm magnification power.
- Mirror;ruler;loads of different masses.
- Screen
- Digital camera with resolving power 7.1 Megapixel.
- Computer,having Linux Version,with GIMP software.
- The sample used in this experiment is a rubber (sponge like) with thickness 0.70mm and length 5.90cm.

4.2 Experimental Setup

The experimental arrangement performed to obtain the moiré fringes is shown in Fig 4.1.

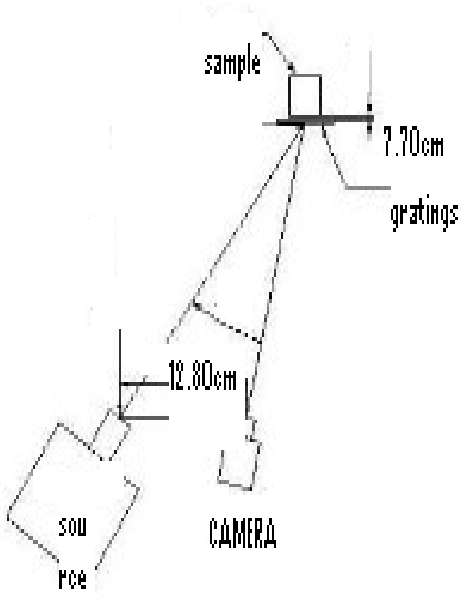

Figure 4.1: Experimental arrangement

The following measurements were done before the setup completed.

- Measuring the separation and length of the gratings
- Calculating the angle between the gratings.
- Adjusting the separation between the Laser source and the digital camera.

Figure 4.2: Setup

4.3 Procedure

I. **Fringe Spacing Determination**

He-Ne laser light was projected onto the diffraction gratings; separated by small angle; and a series of straight parallel fringe patterns were observed on the screen. These series straight fringes (Moiré patterns) were seen on each diffraction order.

The fringe spacing determination was done by writing a FORTRAN program for different angles.

II. **Strain Analysis**

A He-Ne laser which can deliver a power of 1mw was sent directly towards a reflecting mirror,which sent the light upwards to the diffraction gratings of the same 100 lines per mm pitches. Since there was a small angle separation between the two gratings, a series of moiré fringes with different diffraction order has been observed on the sample, which was adjusted above the gratings.

The movement of the diffraction orders were followed while applying loads on the test section.

The mounted, adjusted from below, digital camera captured the first position, i.e. without any load; of these patterns. The first load was put on the sample and again the camera has taken the positions of these fringes. These procedures have been done for 5 different loads. The captured moiré fringes were inputted to a computer. GIMP software was used for pixel to pixel distance measurements; using gray transformation, and for cropping the test area.

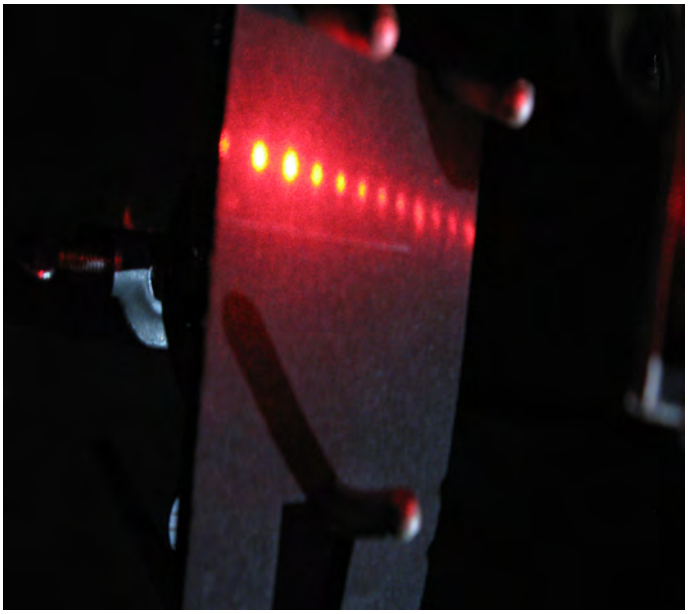

Figure 4.3: Illuminated rubber section

Chapter 5

Results and Discussion

5.1 Data

Length of Test section=5.90cm
Height of Test section=3.20cm
Separation between Camera and Source=12.80cm
Separation of gratings=7.70cm
Angle between gratings=7.38^0
Part I
The two gratings have 100 lines/mm and 300 lines/mm pitches.
Thus; For the first grating(100 lines/mm):
λ_1=1/100 mm [Line spacing of the first grating] and
For the second grating(300 lines/mm):
λ_2=1/300 mm [Line spacing of the second grating]

After compiling the written fortran program for determination of fringe spacing, the following result was obtained.

Table 1: Angular Grating Separation Vs Fringe spacing

alpha(in rad)	spacing(mm)
0.0	0.0050000004
0.1	0.004927837
0.2	0.0047312486
0.3	0.004456986
0.4	0.0041538654
0.5	0.0038571525
0.6	0.0035863332
0.7	0.0033493815
0.8	0.0031476642
0.9	0.002979401
1.0	0.0028416575
1.1	0.002731359

Part II

Table 2:Diffraction pattern Positions without load: crop dimension 1332x504 pixels

Order	X value(pixel)	$\Delta X(pixel)$
1	60	156
2	216	144
3	360	120
4	480	104
5	584	92
6	676	92
7	768	88
8	856	80
9	936	76
10	1012	84
11	1096	80
12	1176	sum1=1116

Figure 5.1: Diffraction fringe patterns before load applied

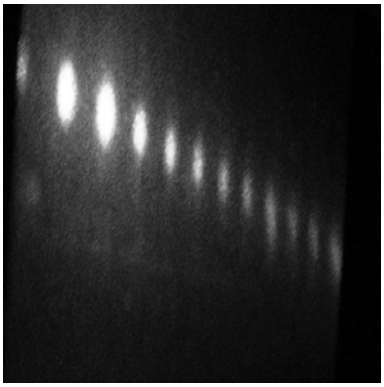

Figure 5.2: GIMP processed diffraction Patterns before load applied

Table 3: Diffraction pattern positions with Load of F=0.98N; Crop Dimension 1332x552

Order	X Value(pixel)	$\Delta X(pixel)$
1	68	172
2	240	148
3	388	128
4	516	112
5	628	104
6	732	96
7	828	92
8	920	92
9	1012	88
10	1100	76
11	1176	80
12	1256	sum6=1188

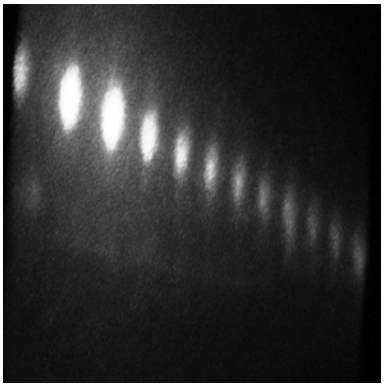

Figure 5.3: GIMP processed diffraction patterns after the last load applied

5.2 Data Analysis

Length of test rubber=5.90 cm =1116 pixels.
Thus : 1 cm = 189.20 pixels.
Area of test section=$5.90cm * 3.20cm = 18.88cm^2 = 1.89 * 10^{-3}m^2$
$\lambda_{beat} = \frac{\lambda_1 * \lambda_2}{\lambda_1 - \lambda_2}$
Hence: $\lambda_{beat} = 0.005000mm$
When we plot the data obtained for fringe spacing against separation of gratings, we get the following graph.

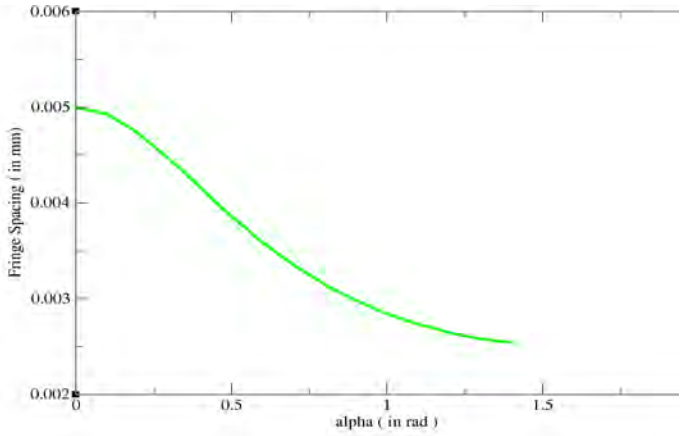

Figure 5.4: Fringe spacing Vs angular separation of gratings

Table 4:Strain Vs Stress values

Strain	Stress (N/m^2)	Elasticity of Modulus (N/m^2)
0.012	84.7	7058.34
0.014	98.8	7057.14
0.016	112.9	7056.25
0.018	127.0	7055.56
0.0502	243.39	4048.40
0.0511	288.37	5643.25
0.0512	324.7	6341.79
0.0521	372.5	7149.71
0.054	394.7	7309.26
0.061	430.2	7052.46
0.062	439.03	7081.13
0.063	473.1	7509.52
0.064	520.1	8126.56

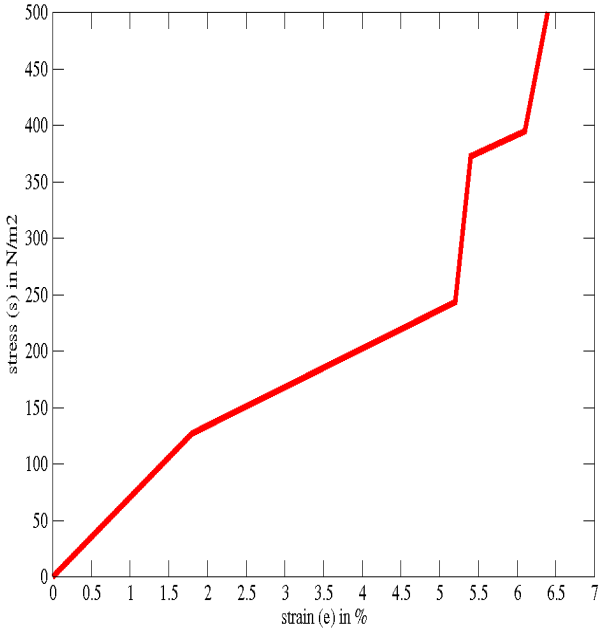

Figure 5.5: Experimentally determined small Strain Stress Behavior of rubber sample

Table 5: Stress and Stretch Ratio Values

Stretch Ratio(λ)	Stress(N/m^2)
1.00	0.0
1.02	127.0
1.05	243.0
1.054	372.49
1.06	394.71
1.065	520.1

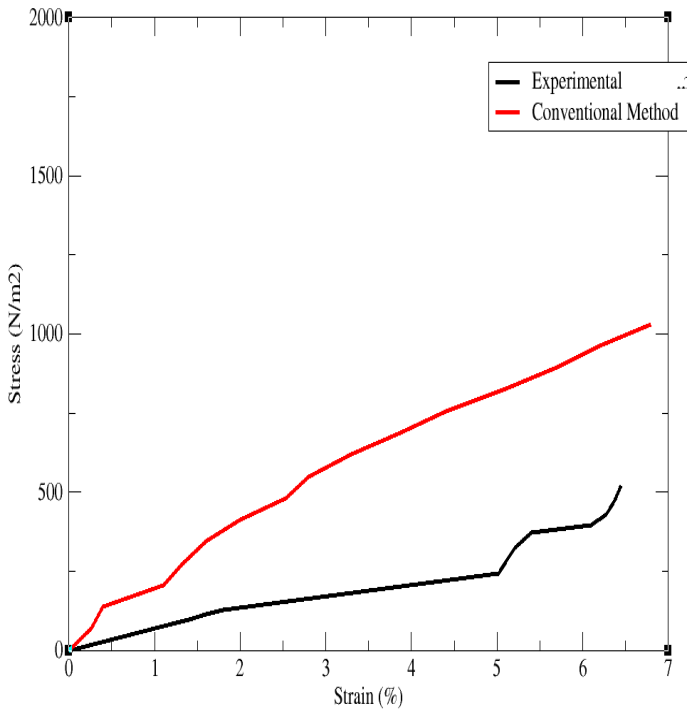

Figure 5.6: Stress Strain behavior of rubber using Moiré technique and Universal Testing Machine

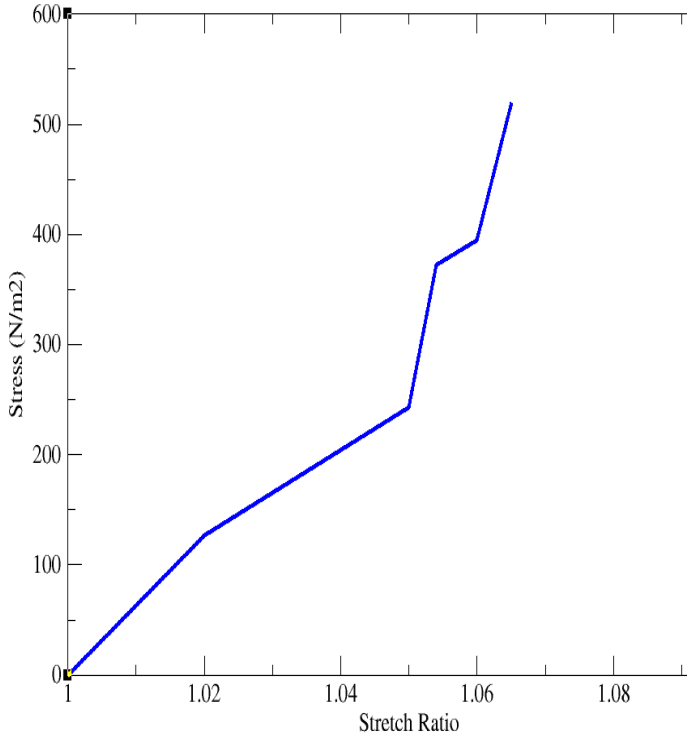

Figure 5.7: Small Stretch Ratio (λ) Vs Stress of the sample

5.3 Discussion

As can clearly be seen from the graph of Fig.5.4; the distance between fringes decreases as the separation between the diffraction gratings increases (for small angles). But for large angles of about 1.58 rad or more, the fringe spacing starts increasing with increase of separation and again decreases after a while as shown in Fig 5.8. For small angles, the data obtained is in agreement with the theory predicted in chapter two. It is also confirmed that when the gratings, 100 lines/mm and 300 lines/mm pitches, are parallel, the fringe spacing equals 0.005000 mm. This is exactly equal to the value obtained for λ_{beat} .

Besides; when $\lambda_1 = \lambda_2$ with $\alpha \neq 0$, the separation between two consecutive bright/dark fringes is $\lambda/2\sin\alpha$.

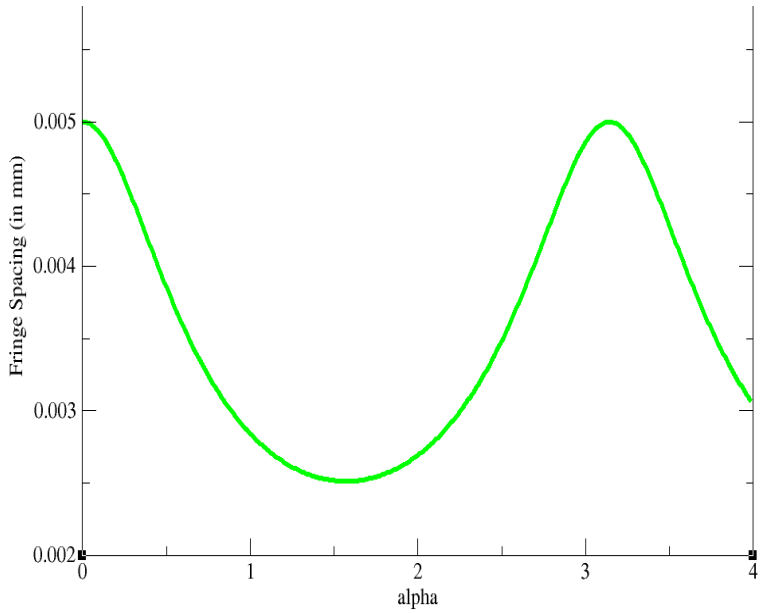

Figure 5.8: General variation of Fringe Spacing

From graphs of Fig.5.5 and Fig.5.6 we infer that the experimentally determined stress strain behavior of rubber is showing similar behavior as the behavior shown in Fig.3.7 at low strain values. It suddenly changes its strain stress curve after the application of the first load.The behavior determined using universal testing machine also confirms the non linear behavior of the sample. Thus, it is in agrement with the theoretically predicted behavior of elastomers described in chapter 3.

5.4 Error Analysis

Each measurement taken in this work is subjected to precision and systematic errors. The weights were measured using beam balance of least scale 0.01g. Thus error expected is $(measured \pm 0.001)g$. Similarly, the length and height of test section measured using ruler have uncertainty of $(5.90 \pm 0.005)cm$ and $(3.20 \pm 0.005)cm$ respectively; separation of gratings (7.70 ± 0.005); separation between camera and source (12.80 ± 0.005). Moreover, the loads were applied on the sample manually and we were limited to take large values of data. And hence, it was not possible to generalize the total stress strain behavior of the sample.

5.4.1 Propagation of Error

Propagation of error (uncertainty) is the effect of variables' uncertainties on the uncertainty of a function based on them. Most commonly, the error on a quantity , ΔX, is given as the standard deviation, σ. Standard deviation is the positive square root of variance, σ^2. The value of a quantity and its error are often expressed as $X \pm \Delta X$. Any non-linear function; f(a,b), of two variables a and b can be expanded as:
$f = f^0 + \frac{\partial f}{\partial a}a + \frac{\partial f}{\partial b}b$; where f^0 is a constant that doesn't contribute to the error on f.
Hence:$\sigma_f^2 = (\frac{\partial f}{\partial a})^2\sigma_a^2 + (\frac{\partial f}{\partial b})^2\sigma_b^2$ Or
$(\frac{\sigma_f}{f})^2 = (\frac{\sigma_a}{a})^2 + (\frac{\sigma_b}{b})^2$
Given the measured variables with uncertainties as $x \pm \Delta x$ and $y \pm \Delta y$; if we want to compute $z = \frac{x}{y}$ with its uncertainty Δz,then:
$\Delta z = z * \sqrt{(\frac{\Delta x}{x})^2 + (\frac{\Delta y}{y})^2}$.
Thus the relative error is:
$\frac{\Delta z}{z} = \sqrt{(\frac{\Delta x}{x})^2 + (\frac{\Delta y}{y})^2}$

Therefore, based on the above analysis, the computed functions in our experiment take the form:
Area of test sample=$(18.8 \pm 0.06)cm^2$
Weight of the masses=$(Calculated \pm 0.03)N$
Stress=$(Calculated \pm 0.1)\frac{N}{m^2}$
Strain=$Calculated \pm 0.0009$
Modulus of Elasticity=$(Calculated \pm 0.05)\frac{N}{m^2}$

5.5 Conclusion and Recommendation

5.5.1 Conclusion

Based on the Moiré technique, the fringe spacings between consecutive bright or dark fringes for different gratings separation are determined. For the special cases; i.e when the separation between the gratings,100 lines/mm and 300 lines/mm pitches, is zero, the fringe spacing equals 0.005000 mm. This is exactly equal to the value for λ_{beat}.
Besides; when $\lambda_1 = \lambda_2$ with $\alpha \neq 0$, the separation between two consecutive bright/dark

fringes is $\lambda/2\sin\alpha$.
The experimentally determined behavior shows that at small strain values, the rubber test sample changes its strain stress curve radically after the first application of the load. This is in agreement with the theory showed in chapter 3. Thus, Moiré fringe projection technique can be used for deformation measurement.

5.5.2 Recommendation and Future outlook

As our country is attracting investors to invest in industry related activities, the need of technical support in the area is unquestionable. From this research we concluded that a more advanced Moiré technique is suitable for deformation measurement. Especially if the loading mechanism was designed using computer and the fringes were observed using better camera; an excellent result could be obtained. Thus, industries, like rubber and plastic factories, could use this technique for easy, reliable deformation measurements. Moreover; we would like to recommend that this technique can be used in universities for graduate level laboratory sessions.

The fringes produced by sliding (stretch) and rotation of one grating over the other are assumed to be independent. A simulation technique which can demonstrate this decoupled phenomena is the future plan in the area.

Appendix A

Deformation, D, is calculated as the difference between the final length of the material reached due to the loads and the original length of the material, i.e. without load.
Thus:
The deformation occurred due to $F_1 = 0.24N$ is
$D_1 = sum2 - sum1$=(1136-1116) pixels =20 pixels.
The deformation due to $F_2 = 0.46N$ is
$D_2 = sum3 - sum1 = 1172 - 1116 = 56pixels$
The deformation due to $F_3 = 0.70N$ is
$D_3 = sum4 - sum1 = 1176 - 1116 = 60pixels$
Due to $F_4 = 0.75N$ is
$D_4 = sum5 - sum1 = 1184 - 1116 = 68pixels$
And finally the deformation occurred due to $F_5 = 0.98N$ is
$D_5 = sum6 - sum1 = 1188 - 1116 = 72pixels$
Now the normal (engineering) strain, e, is given by the ratio of deformation occurred to the original length of the test section.
Hence:
$e_1 = \frac{D_1}{sum1} = 0.0180$
$e_2 = \frac{D_2}{sum1} = 0.0502$
$e_3 = \frac{D_3}{sum1} = 0.0540$
$e_4 = \frac{D_4}{sum1} = 0.0610$ And
$e_5 = \frac{D_5}{sum1} = 0.0645$
Stress is the applied force per unit area of the test section.
i.e.
$s_1 = \frac{0.24N}{1.89*10^{-3}m^2} = 127.0\frac{N}{m^2}$
$s_2 = \frac{0.46N}{1.89*10^{-3}m^2} = 243.39\frac{N}{m^2}$
$s_3 = \frac{0.704N}{1.89*10^{-3}m^2} = 372.49\frac{N}{m^2}$

$s_4 = \frac{0.746N}{1.89*10^{-3}m^2} = 394.71\frac{N}{m^2}$
$s_5 = \frac{0.983N}{1.89*10^{-3}m^2} = 520.10\frac{N}{m^2}$
The modulus of elasticity , E, is found by $E = \frac{S}{e}$; where S is the stress and e is the corresponding strain.
Hence for the first portion of the graph of Fig.5.5;
$E_1 = \frac{S_1}{e_1} = 7058.34\frac{N}{m^2}$
$E_2 = \frac{S_2}{e_2} = 7057.14\frac{N}{m^2}$
$E_3 = \frac{S_3}{e_3} = 7056.25\frac{N}{m^2}$
$E_4 = \frac{S_4}{e_4} = 7055.56\frac{N}{m^2}$
Thus the representative modulus of elasticity for the first portion is:
$\overline{E} = \frac{E_1+E_2+E_3+E_4}{4} = 7056.82\frac{N}{m^2}$
For the second portion of the graph of Fig.5.5;
$E_5 = \frac{S_5}{e_5} = 4848.41\frac{N}{m^2}$
$E_6 = \frac{S_6}{e_6} = 5643.25\frac{N}{m^2}$
$E_7 = \frac{S_7}{e_7} = 6341.80\frac{N}{m^2}$
$E_8 = \frac{S_8}{e_8} = 7149.71\frac{N}{m^2}$
$E_9 = \frac{S_9}{e_9} = 7309.26\frac{N}{m^2}$
Thus the representative modulus of elasticity for second portion is:
$\overline{E} = 6258.49\frac{N}{m^2}$
For the third portion of the graph of Fig.5.5;
$E_{10} = \frac{S_{10}}{e_{10}} = 7052.46\frac{N}{m^2}$
$E_{11} = \frac{S_{11}}{e_{11}} = 7081.13\frac{N}{m^2}$
$E_{12} = \frac{S_{12}}{e_{12}} = 7509.52\frac{N}{m^2}$
$E_{13} = \frac{S_{13}}{e_{13}} = 8126.56\frac{N}{m^2}$
$E_{14} = \frac{S_{14}}{e_{14}} = 8126.56\frac{N}{m^2}$
Thus the representative modulus of elasticity for the third portion is:
$\overline{E} = 7442.42\frac{N}{m^2}$
The strain energy per unit volume of the sample up to 0.018 strain value is calculated as:
$U = \sum_{i=1}^{5} S_i * e_i$
Hence:
$U = 0 + 1.02 + 1.38 + 1.81 + 2.29$
$= 6.50\frac{J}{m^3}$.
This is to mean that, the material absorbs 6.50J of energy, without suffering damage,

in straining up to 0.018. Conversely, if we unload the material from this strain position, it uses 6.50J reversible energy to come to the material's original position.

The stretch ratio or extension ratio , λ, is a measure of the extensional or normal strain of a differential line element, which can be defined at the undeformed configuration. It is defined as the ratio between the final length, l, and the initial length,L, of the material line.

Thus:

$\lambda = l/L$

Now:

$\lambda_1 = \frac{l_1}{L} = 1136/1116 = 1.02$

$\lambda_2 = \frac{l_2}{L} = 1172/1116 = 1.05$

$\lambda_3 = \frac{l_3}{L} = 1176/1116 = 1.054$

$\lambda_4 = \frac{l_4}{L} = 1184/1116 = 1.06$

$\lambda_5 = \frac{l_5}{L} = 1188/1116 = 1.065$

Appendix B

A. Program fringespacing

```
**********************************************************************
!This program determines the fringe spacing created by
!Moire technique for the general case (case 3).
!It also compares the special cases for alpha=0 and/or l1=l2
! © Setegn Ayalew Bogale
**********************************************************************
! Input Arguments:
! l1 - line spacing of grating1 in mm (100 lines/mm)
! l2 - line spacing of grating2 in mm (300 lines/mm)
! lbeat - the beat wavelength between gratings
! alpha-angle separation of gratings
! C-fringe spacing
**********************************************************************
real::c,alpha,l1,l2,k,h,s,m,n,p,q,lbeat
integer::i
open(unit=1,file="output.dat",status="unknown")
l1=1.0/100.0 !line spacing of grating1 in mm (100 lines/mm)
l2=1.0/300.0 !line spacing of grating2 in mm (300 lines/mm)
h=0.01 !step size
lbeat=(l1*l2)/abs(l2-l1) !This value is exactly the same as c when
alpha=0
!print*,"beat wave length",lbeat
!call subroutine sub()
!contains
!subroutine sub()
```

```
alpha=-0.01 !in radian
do i=1,400
!alpha=0!in radian
alpha=alpha+h
k=l1*l2
m=l2**2*sin(2*alpha)**2
n=(l2*cos(2*alpha)-l1)
q=n**2
p=m+q
c=k/sqrt(p) !fringe spacing
if( alpha >= 30)exit
write(1,*)alpha,c
!print*,n,q,p,c
end do
!end subroutine sub
end program fringespacing
```

!B.program beat

```
implicit none
**************************************************************************
!This program determines the fringe spacing created by
!Moire technique for the case l1=l2.
!© Setegn Ayalew Bogale
**************************************************************************
real::l1,l2,l,alpha,h
integer::i
l1=0.02
alpha=0
h=1
do i=1 ,16
alpha=alpha+h
l=l1/abs(2*sin(alpha))
!l=(l1*l2)/abs(l2-l1)
print*,l
end do
end program beat
```

C. program curve

```
**********************************************************************
!This program is used for curve fitting of strain vs stress
!© Setegn Ayalew Bogale
**********************************************************************
implicit none
real,dimension(6)::x,f
real::xo,product1,sum1
integer::j,k
SAVE x,f
DATA x/0.0,0.018,0.0502,0.054,0.061,0.0645/
DATA f/0.0,127.00,243.39,372.49,394.71,520.10/
sum1=0
xo=0.025
!allocate(pnj)
!allocate(x(j))
!allocate(x(k))
!allocate(f(j))
do j=1,6
product1=1
do k=1,6
if(k/=j)then
product1=product1*(xo-x(k))/(x(j)-x(k))
end if
end do
!if(x>5)exit
sum1=sum1+f(j)*product1
end do
print*,xo,sum1
!deallocate(pnj)
!deallocate(x)
!deallocate(x)
!deallocate(f)
end program curve
```

Appendix C

Table 6:Loads applied

mass(in g)	Weight(in N)
24.51	0.24
46.74	0.46
70.45	0.70
74.66	0.75
98.37	0.98

Table 7: Diffraction pattern Positions with Load of F=0.24N; Crop Dimension 1332x580

Order	X value(pixel)	$\Delta x(pixel)$
1	88	160
2	248	144
3	392	120
4	512	116
5	628	100
6	728	92
7	820	84
8	904	92
9	996	68
10	1064	80
11	1144	80
12	1224	sum2=1136

Table 8:Diffraction pattern Positions with Load of F=0.46N; Crop Dimension 1332x641

Order	X value(pixel)	$\Delta X(pixel)$
1	64	168
2	232	148
3	380	132
4	512	108
5	620	100
6	720	100
7	820	92
8	912	80
9	992	88
10	1080	80
11	1160	76
12	1236	sum3=1172

Table 9: Diffraction pattern Positions With Load of F=0.704N; Crop Dimension 1332x555

order	X Value(pixel)	$\Delta X(pixel)$
1	76	172
2	248	148
3	396	128
4	524	112
5	636	104
6	740	92
7	832	88
8	920	92
9	1012	84
10	1096	84
11	1180	72
12	1252	sum4=1176

Table 10: Diffraction pattern Positions with Load of F=0.746N; Crop Dimension 1332x562

Order	X value (pixel)	$\Delta X(pixel)$
1	64	172
2	236	140
3	376	132
4	508	116
5	624	100
6	724	100
7	824	92
8	916	88
9	1004	80
10	1084	88
11	1172	76
12	1248	sum5=1184

Bibliography

[1] Lord Rayleigh *On the manufacture and theory of diffraction gratings*,Scientific Papers,1,209;Phil.Mag.47,81-93

[2] Guild J. *The interference systems of crossed diffraction Gratings;Theory of moire fringes*,The National Physical Laboratory,Oxford 1956,.

[3] C.J.Ball *An Introduction to the theory of diffraction*,Pergamon Press,Oxford Christopher Palmer *Diffraction Gratings;the crucial dispersive component* Rochester 1995,Newyork.

[4] D.Pallek,K.A Butefisch *Model Deformation Measurement In ETW Using The Moiré Technique* ,Institute of Aerodynamics and Flow Technology,Gottingen,Germany 2002.

[5] D.Albiero,S.Rodrigues *Determination of wood specimens using isostrain patterns generated for moiré technique*,International congress of Agricultural engineering,2004,Leuven,Belgium,p.612-700.

[6] Yinyan Wang and Patrick Hassel, *Measurement of Thermally Induced Warpage of BGA packages/substrates using Phase stepping Shadow Moire*,Electronic Packaging Services;430 Tenth Street,suite 2002,Atlanta,GA 30318

[7] Mitsuo Takeda,et al *Fourier transform method of fringe pattern analysis for computer based topography and interferometry*, Journal of the Optical Society of America,Vol.72,No.1/January 1982.

[8] Song Yaozu,Zhang Xiangchun,Zhang Honglin "Laser Moiré Deflectometry Applicable for Mini/Micro scale Flow Visualization".,Optical Technology and Image Processing for Fluids and solids Diagnostics 2002.SPIE Vol.5058(2003)

[9] International Standard , *Determination of tensile properties*,ISO 572-2:1993(E)

[10] K.Creath and J.c Wyant, *Moiré and Fringe Projection Technique*,second edition,Optical Shop Testing,ISBN 0-471-52232:1992,John Wiley and Sons.inc.

[11] Krishna C. Baranwal and Howard Stephens,*"Basic Elastomer Technology," Rubber Division*,American Chemical Society, University of Akron, Akron, OH, 2001.

[12] Meadows,D.M.W,O.Johnson,and J.B.Allen,*"Generation of Surface Contours by Moiré patterns"*Appl.Opt.9(4),942-947(1970)

[13] Der Hovanesian J. and Y.Y.Yung,*"Moiré Contour Sum Contour difference,and vibration analysis of arbitrary objects"*Appl.Opt.10(12),2734-2738(1971).

[14] Chiang F.P,*Moiré Methods of Strain Analysis,in Manual on Experimental Stress Analysis*,Brookfield Center,CT,1983,pp.51-69.

[15] David Roylance,*Stress Strain Curves*,Massachusetts Institute of Technology Cambridge,MA 02139(2001)

[16] Lawrence E., *Mechanical Properties of Polymers and Composites*,second edition,pp.412-414.

[17] James E. Mark, Burak Erman, and Frederick R, Erich,*"Science and Technology of Rubber"*Academic Press, San Diego, CA, 1994.

[18] Gary Cloud,*Optical Methods in Experimental Mechanics;"Geometric Moiré Phenomena and Simulations"*,Michigan State University,Parts 18-21.

[19] Wolfram.com,*Experimental Errors and Error analysis*,http://documents.wolfram.com/applications/eda/experimentalerrorsandanalysis.html

[20] Wikipedia the free encyclopedia, *Stress Strain Analysis*